

Overwinter sea-ice characteristics important for Antarctic krill recruitment in the southwest Atlantic



Devi Veytia ^{a,*}, Sophie Bestley ^{a,b}, So Kawaguchi ^{b,c}, Klaus M. Meiners ^{b,c}, Eugene J. Murphy ^d, Alexander D. Fraser ^b, Kazuya Kusahara ^e, Noriaki Kimura ^f, Stuart Corney ^a

^a Institute for Marine and Antarctic Studies, University of Tasmania, 20 Castray Esp., Hobart, Tasmania 7000, Australia

^b Australian Antarctic Program Partnership, Institute for Marine and Antarctic Studies, University of Tasmania, Hobart, Tasmania 7004, Australia

^c Australian Antarctic Division, Department of Agriculture, Water and the Environment, 203 Channel Highway, Kingston, Tasmania 7050, Australia

^d British Antarctic Survey, High Cross, Madingley Road, Cambridge CB3 0ET, UK

^e Japan Agency for Marine Earth Science and Technology (JAMSTEC), Yokohama, Kanagawa 236-0001, Japan

^f Atmosphere and Ocean Research Institute, The University of Tokyo, 5-1-5 Kashiwanoha, Kashiwa 277-8568, Japan

ARTICLE INFO

Keywords:

Climate change

Sea ice

Antarctic krill

Euphausia superba

Overwinter survival

Recruitment

ABSTRACT

Climate change alters the extent and structure of sea-ice environments, which affects how they function as a habitat for polar species. Identifying sea-ice characteristics that serve as indicators of habitat quality will be crucial to the monitoring and management of climate change impacts. In the Southern Ocean, Antarctic krill is a key prey species and fishery target. Krill larvae depend upon sea-ice habitats to survive the winter and recruit to the population in spring. Existing observations of sea-ice characteristics lack sufficient spatiotemporal coverage to quantify which ones contribute to favourable overwintering habitat, leading to uncertainties in how current and future changes in sea ice affect krill populations. Here, we derive regional-scale indices of annual krill recruitment spanning 35 years across the southwest Atlantic. To develop meaningful indicators of sea-ice habitat, we selected variables from a high-resolution sea-ice model that are hypothesized as relevant for larval habitat use. The resulting correlations between recruitment and sea-ice indicators vary by region and show remote connections to sea ice that correspond with established theories of larval transport. Through an improved representation of sea-ice habitat quality, as compared with using more traditional satellite-derived variables such as sea-ice extent and duration, we highlight plausible regions of overwintering habitat. Our findings improve current understanding of how krill are likely responding to changing sea ice and support emerging views that larval habitat use is complex. Furthermore, regional variation in larval dependence on sea ice may provide pockets of resilience to change for the broader krill population.

1. Introduction

Sea ice is highly sensitive to global warming with profound consequences for polar species and ecosystems (Maksym, 2019; Meredith et al., 2019). As many management strategies rely on the capacity to quickly diagnose ecosystem state, identifying indicators of sea-ice habitat quality is a priority. Developing these sea-ice indicators would require quantifying how variation in sea-ice characteristics determines habitat quality for dependent species.

In the Southern Ocean, Antarctic krill (*Euphausia superba*, hereafter krill) are an integral part of the marine ecosystem and are dependent on sea ice during their early life stages. They are a primary prey source

supporting a diverse assemblage of marine predators including whales, seals, penguins and flying seabirds (Murphy et al., 2007a, 2016; Trathan and Hill, 2016). They also play a role in nutrient cycling (Cavan et al., 2019; Schmidt et al., 2011) and are the target of the Southern Ocean's largest (and growing) fishery (Nicol and Foster, 2016).

Environmental variation, including sea-ice variability, drives large fluctuations in krill biomass on regional and interannual scales (Murphy et al., 2007b), which exerts a bottom-up control on the population dynamics of local and migratory dependant predators (Croxall et al., 1999; Trathan and Hill, 2016). Krill recruitment (*i.e.* the survival of larvae until they are one year old) is likely a significant driver of interannual krill abundance and population dynamics (Murphy et al., 1998; Quetin

* Corresponding author.

E-mail address: devi.veytia@utas.edu.au (D. Veytia).

and Ross, 2003; Siegel and Loeb, 1995). Quantifying the drivers of krill recruitment variability is therefore of key importance to understanding ecosystem-level impacts of climate variability and change, as well as informing conservation measures in the Southern Ocean.

Overwinter survival is thought to constrain krill recruitment (Atkinson et al., 2004; Siegel and Loeb, 1995). Larval krill feed primarily on phytoplankton and cannot survive prolonged periods of starvation (Yoshida et al., 2009), yet in winter pelagic phytoplankton growth is severely limited by light, caused by the high latitude, sea-ice cover and deep vertical mixing (Arrigo and Thomas, 2004; Boyd, 2002). Sea-ice algae, however, can thrive close to the increased light availability at the top of the water column as well as concentrated nutrients (Arrigo, 2014). Observational studies indicate that krill larvae may have evolved an overwintering strategy reliant on sea-ice habitats. Larvae have been observed scraping sea-ice algae from under-ice surfaces (Hamner et al., 1989) and sea-ice algae have been identified as a critical diet component (Daly, 1990; Ju and Harvey, 2004; Kohlbach et al., 2017; Meyer et al., 2002; Schmidt et al., 2014). Caverns created under ridged sea ice may also provide refuge from currents (Daly, 1990; Meyer, 2012; Meyer et al., 2009). These findings were synthesized into the general conceptual model of sea ice functioning as an important foraging substrate and refuge to support overwinter larval survival (Nicol, 2006).

Emerging studies find regional plasticity in larval reliance on sea ice. In the Weddell Sea, larval diets were found to be composed of heterotrophic and autotrophic components from both the water column and sea ice, and larval growth was maximized in the dynamic marginal ice zone (MIZ) rather than the interior pack ice as previously thought (Meyer et al., 2017). Results from other diet studies show that larvae can opportunistically feed on dietary sources from the water column (both under the sea ice and in the open ocean) to meet their energetic requirements (Daly, 1990, 2004; Jia et al., 2016; Walsh et al., 2020).

From a mechanistic perspective, local-scale studies indicate that sea-ice habitat quality may be characterized by a range of variables: thickness and snow cover to optimize the growth of sea-ice bottom algae communities (Jeffery et al., 2020; Meiners et al., 2012; Wongpan et al., 2018), ridging (*i.e.* deformed sea ice) to provide refuge, and dynamism, as seen in the MIZ (Massom et al., 2006; Meyer et al., 2017). In addition, at large scales larvae are likely advected as passive drifters over winter. The most recent theory regarding larval overwinter transport is that larvae are advected in association with sea ice during the day and with surface currents at night (Meyer et al., 2017). If sea-ice characteristics are indicators of habitat quality, then recruitment measured in the spring/summer would be related to sea ice along the preceding winter's transport pathways (Kohlbach et al., 2017). The environmental conditions that determine larval overwinter habitat therefore operate over large spatiotemporal scales. However, these theories are based on local-scale studies and cannot be confidently extrapolated to define larger-scale relationships. While mesoscale sea ice sampling methods using autonomous underwater vehicles or under-ice trawls as well as aerial observations provide an important stepping stone to link local studies to broader scales of inquiry (e.g. Castellani et al., 2020; David et al., 2016; Flores et al., 2012; Schaafsma et al., 2016), achieving the necessary large-scale spatiotemporal characterisation of relevant sea-ice variables requires satellite remote sensing.

Until recently, sea-ice concentration (SIC) was the most widely used remotely sensed sea-ice characteristic, likely due to its good daily temporal coverage and validation. More dynamically driven sea-ice characteristics (such as deformations created from ridging, snow-cover, and swell) are difficult to detect remotely with legacy instruments. Large-scale maps of variables such as thickness have been interpolated from networks of *in-situ* measurements (Worby et al., 2008). However, interpolation cannot provide sufficient accuracy and temporal resolution for the purposes of ecological modelling, and these measurements are time-consuming and costly to collect. While technologies to obtain remote measurements of other sea-ice characteristics such as thickness and snow cover are in their nascent stage, the time series of these

measurements is not as long.

A shortened record of satellite data can reduce statistical power to detect relationships with krill recruitment. Recruitment indices across larger scales are calculated from net tow data, which are compiled opportunistically using the KRILLBASE databases (Atkinson et al., 2017). This results in a noisy time series that is fragmented in space and time. To detect a signal across a noisy time series, increased statistical power and thus length of time series is needed. These restrictions influence the scope of studies quantifying the effects of changing sea ice on recruitment.

Past analyses have been based on SIC and SIC-derived variables such as sea-ice extent (SIE), timing of advance (TOA), duration (DUR) and timing of retreat (TOR) (Stammerjohn et al., 2008; see Table 1 for commonly used abbreviations). From these, declining SIE (Atkinson et al., 2004; Kawaguchi and Satake, 1994; Mackintosh, 1972; Nicol et al., 2000; Quetin et al., 2007; Siegel and Loeb, 1995), timing (Piñones and Fedorov, 2016; Quetin et al., 2007), as well as larger-scale climate modes that influence sea-ice dynamics, such as the Southern Annular Mode (SAM) (Atkinson et al., 2019; Saba et al., 2014) and El Niño Southern Oscillation (ENSO) (Loeb and Santora, 2015) have been identified as influential for krill recruitment.

The mechanisms that underpin the relationships between recruitment and these sea-ice variables remain unclear. This gives us low confidence that these relationships will be maintained into a future driven by climate change (Cox et al., 2018; Saba et al., 2014). For example, extrapolating the relationship between krill density and SIE leads to a grim outlook for long-term krill population trajectories as circumpolar SIE is projected to decrease by ~ 30% by 2100 (Maksym, 2019). However, when sea-ice thickness (SIT) and ridging rate (RR) are accounted for in projections, suitable larval habitat may indeed expand in the future (Melbourne-Thomas et al., 2016). To refine our hypotheses of how krill will respond to these variables in a changing climate, we need to quantify relationships between recruitment variability and sea-ice variables that reflect a more mechanistic understanding of habitat use and quality.

Here, we use a sea-ice model to explore relationships between indicators of sea-ice habitat quality and krill recruitment in the southwest Atlantic. This approach is useful for testing hypotheses on environmental drivers of population dynamics within a quantitative framework. Our motivation is for this study to compliment and inform the application of existing and emerging satellite products. To do this, we first develop a time series of regional-scale krill recruitment indices from krill density and length frequency data from net tows. This time series incorporates data spanning 35 years and resolves the entire southwest Atlantic – the population centre for krill (Atkinson et al., 2004) – at a regional scale. We also derive a suite of modern sea-ice indicators

Table 1
Commonly used abbreviations.

Category	Abbreviation	Long Name
Sea-ice variables	SIE	Sea-ice extent
	MIZ	Marginal Ice Zone
	SIC	Sea-ice concentration
	RR	Ridging rate
	SIT	Sea-ice thickness
	DUR	Sea-ice duration (Stammerjohn et al., 2008)
	TOA	Sea-ice time of arrival (Stammerjohn et al., 2008)
	TOR	Sea-ice time of retreat (Stammerjohn et al., 2008)
	sd	Standard deviation
	cv	Coefficient of variation
	max	Maximum
Geographical and oceanographic features	ACC	Antarctic Circumpolar Current
	wAP	western Antarctic Peninsula
	AP	Antarctic Peninsula

Table 2

Ecological significance and derivation of modern sea-ice indicator variables. All variables were calculated from model estimates of SIC, SIT or RR (daily timesteps).

Variable Name	Calculation Method	Ecological Significance
Jul-Aug max RR	The maximum daily value of RR, calculated from all the days in July and August of each year.	In July–August light remains too low to support photosynthesis, and therefore it is unlikely that sea ice supports a high enough ice algal bottom community growth to sustain larval krill (Meiners et al., 2012; Meyer, 2012, Fig. 5). This is supported by the low larval growth rates observed during midwinter (Supplementary Table 1 in Meyer et al., 2017). Rather, sea ice likely functions as a refuge. This would be characterized by over-rafterd ice that provides a three-dimensionally complex environment for krill to shelter from predators and currents (Meyer et al., 2009). Maximum RR is considered a better indicator of over-rafterd ice rather than mean RR, as a large ridging event (e.g. a storm) would create the over-rafterd structures that would then persist for some time.
Jul-Aug mean-mode SIT	The mean minus the mode values of SIT, calculated from all the days in July and August of each year.	This metric serves as an additional approximation of deformed ice. The higher the difference of mean and mode thickness, the more the thickness distribution of ice has a right skew, indicating a higher degree of deformation and presence of thicker ridged ice (Haas, 2004). In a previous study, larvae were found to be abundant under ice with a high mean-mode (termed ice type 1) in both the pack ice and MIZ (Meyer et al., 2017). While in the previous study mean-mode was derived from spatial measurements, in this study the metric is calculated over time. We hypothesize that this approach is still valid, as ice that is highly deformed over time would likely also be deformed spatially.
Sep MIZ coverage	The percentage of days in September that a grid cell was classified as MIZ using the thresholds identified in the sensitivity analysis.	In September, when there is more light to support ice algal growth (Meiners et al., 2012), we expect the most important ice qualities to be those that favour the creation of a structurally complex, food-rich habitat for krill to feed. Some observational evidence indicates that the MIZ, which is estimated to have some of the largest ice algal concentrations (Arrigo et al., 1997), provides a superior grazing habitat for krill (Brierley et al., 2002; Meyer et al., 2017). Similarly to the MIZ, ice that supports higher food availability is likely dynamic, as processes such as grinding may release ice algae into the water column, making it more accessible (Meyer et al., 2017; Walsh et al., 2020).
Sep sd RR	The sd of all the daily values of September RR, calculated for each year.	SIT likely has a complex relationship with krill habitat quality. While excessively thick ice would attenuate the light available to sea ice bottom algal communities, maintaining a certain amount of thickness is likely key to optimizing habitat. Both algal bottom communities and larval grazing substrate would be maximized in thicker, deformed ice (Meiners et al., 2012; Meyer et al., 2017).
Sep mean SIT	The mean of all the daily values of September SIT, calculated for each year.	

(Table 2) relevant to hypothesized mechanisms of sea ice influence on krill recruitment. Since such variables are not available from remote sensing with the requisite temporal coverage, we obtain estimates using output from a high-resolution coupled sea ice-ocean model. Maps of temporal correlations are then evaluated between krill recruitment and the sea-ice indicators, and the results compared with those obtained using more traditional sea-ice variables derived from satellite SIC. Through a more sophisticated representation of sea-ice habitat this study represents the first broad-scale analysis that enables a mechanistic understanding to inform the quantification of sea-ice habitat quality. This provides insight into both contemporary and future environmental drivers of krill recruitment, and hence the status of krill populations and the wider Southern Ocean ecosystem.

2. Methods

2.1. Study area

Our study area (130°W to 25°W and 75°S to 50°S, Fig. 1) covers the southwest Atlantic and its oceanographically upstream regions (*i.e.* the Bellingshausen and Amundsen Seas). The southwest Atlantic contains >50% of the circumpolar krill biomass (Atkinson et al., 2009), which supports a rich community of krill predators (Trathan and Hill, 2016), as well as the entire contemporary krill fishing effort (Nicol and Foster, 2016). This sector also has the best historical spatiotemporal research sampling coverage of net tows (e.g. KRILLBASE; (Atkinson et al., 2017)) providing krill length frequency datasets, which are concentrated along the western Antarctic Peninsula (wAP) and around South Georgia.

2.2. Krill recruit density

2.2.1. Data description: Krill density and length frequency

Both krill density (number of krill under 1 m² of sea surface) and length frequency (histogram of length measurements from individual krill) data were used to develop regional-scale recruitment indices for this study. Krill density data were retrieved from the KRILLBASE density

database (hereafter “the density database”, <https://www.bas.ac.uk/project/krillbase/>), which is a freely-available database comprising net samples of krill over the Southern Ocean. Krill length frequency data were compiled from two sources. The KRILLBASE length frequency database is a similar data rescue project to the density database and comprises krill length frequency measurements, sampled from scientific and commercial hauls. To augment the KRILLBASE length frequency database, we combined its measurements with length frequency measurements from the Palmer LTER study region spanning 2009–2016 (Palmer Station Antarctica LTER and Steinberg, 2020). This combined dataset will hereafter be referred to as “the length-frequency database”.

Since these databases are compiled from uncoordinated scientific cruises spanning a long time period (1926–2016), it is difficult to directly compare measurements that may have been taken with varying sampling methods. To minimize the influence of these differences in our analysis, we use the standardized krill density values which adjust measurements to a standard sampling method (Atkinson et al., 2017). To our knowledge no analogous standardization method exists for the length-frequency data, so no correction is applied.

Measurements from both databases were subsequently filtered and binned to nine equal-area hexagonal polygon grid (green hexagons, Fig. 1). For more details on data filtering, preparation, and binning, see Appendix B.i.

2.2.2. Deriving recruit density

Recruit density is calculated by multiplying the mean krill density for each region and sampling season by the corresponding proportion of 1-year-old krill in the population (R_1) (Atkinson et al., 2019; De la Mare, 1994). Different methods exist to derive R_1 from pooled length frequency data, from classifying any krill measurements with a length between 15 and 30 mm as recruits (Atkinson et al., 2019; Perry et al., 2019), to more complex methods utilising a mixture distribution (e.g. Bhattacharya, 1967; De la Mare, 1994; Macdonald and Pitcher, 1979). We decided to employ a mixture distribution, to recognize that at the regional scale of our analysis growth rates between our regions may vary and generate distinct length frequency distributions. Of the mixture

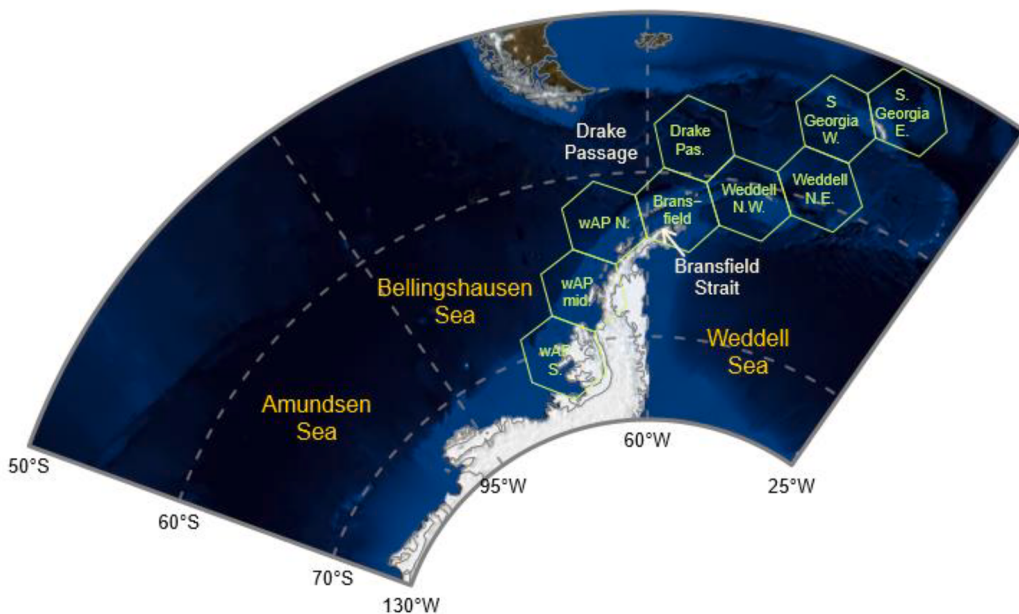


Fig. 1. Map of study area. This map highlights the recruitment regions in which krill density and length-frequency data were binned (green), as well as commonly referenced oceanographic features (white) and seas (yellow). The bathymetry and coastline raster was retrieved from the Blue Marble: Next Generation dataset, produced by the NASA Earth Observatory. (For interpretation of the references to colour in this figure legend, the reader is referred to the web version of this article.)

distribution methods, the Bhattacharya (1967) method has a unique quality in that the number of modes that the distribution fits is informed by the data itself, and not a pre-conceived growth model (which may have unknown regional variations). However, this requires that the user manually selects from the data where these modes occur and this is not entirely objective. We therefore decided to use the number of modes derived using the Bhattacharya (1967) method, along with their corresponding means and standard deviations, to inform a Gaussian mixture distribution (Fig. 2). A resulting mode was determined to be a recruit if the mean was < 33 mm (Siegel, 2000). For each region and sampling season, the R_1 was the sum of the proportions of all modes classified as recruits.

Recruit density for each region and sampling season was then calculated by multiplying the corresponding mean krill density and R_1 values. To validate our new approaches to calculating R_1 , we compared the recruit density derived here with published values. Since existing time series of recruit density are pooled over the southwest Atlantic rather than by region (Fig. S1, Atkinson et al., 2019), a direct comparison of interannual trends was not possible. An approximate comparison was done by fitting a simple log-linear regression to our regional recruit density by sampling season. For this comparison recruit density values to which Palmer LTER data contributed were removed, as these were not included in the Atkinson et al. (2019) time series.

2.3. Evaluating and summarising sea-ice model output

Here, as an initial exploration, we selected a single sea-ice model that has been shown to accurately reproduce key physical sea-ice properties (Kusahara et al., 2018, 2017, 2019). Multi-model ensemble approaches using Intergovernmental Panel on Climate Change (IPCC)-class models (e.g. Veytia et al., 2020) are suitable for broad-brush approaches over larger spatio-temporal time scales, however they are not suitable for our purposes. For this study we require a model, providing daily output for a wide range of sea-ice variables, that has been tuned to represent sea-ice processes in the Southern Ocean. Publicly available IPCC-class models provide monthly output for a range of variables for every region of the Earth. Many of these models do not represent Southern Ocean sea ice accurately (Cavanagh et al., 2017) and even those that do only output a small selection of the possible variables that describe sea ice. Therefore,

our single-model approach is appropriate to address the specific research questions posed in this paper.

2.3.1. Data description: sea-ice model

We obtained estimates of sea-ice concentration (SIC), sea-ice thickness (SIT) and ridging rate (RR) (*i.e.* the rate of sea-ice convergence) from a high-resolution coupled ocean-sea ice model (v4.0, Hasumi, 2006) with an ice shelf component (Kusahara and Hasumi, 2013), hereafter “the model”. The model outputs are the result of a hindcast simulation run from 1979 to 2016, with atmospheric surface boundary conditions from the global atmospheric reanalysis ERA-Interim (Dee et al., 2011). The model uses an irregular grid with a horizontal resolution of 10–20 km in Antarctic coastal margins. Outputs are available in daily timesteps. Previous evaluations conclude that this model can effectively reproduce trends in Antarctic sea-ice extent (SIE) and SIC (Kusahara et al., 2018, 2017, 2019), as well as thickness in autumn – spring (winter was not evaluated) (Kusahara et al., 2019).

The model output was summarised into two sets of sea-ice variables: “classic” and “modern”. Classic variables are traditionally calculated from SIC measurements, such as time of arrival (TOA), time of retreat (TOR) and duration (DUR). Our modern variables reflect sea-ice characteristics hypothesized to be advantageous to larvae (Section 2.3.4). Most of these variables (*i.e.* those that are calculated from SIT or RR) are still new to remote sensing and thus a better temporal coverage can be achieved using estimates from the model. For compatibility with mapping packages, the daily output was remapped onto a regular grid over the study area, with a resolution similar to that of its native grid (14 km), using the lambert azimuthal equal-area projection.

2.3.2. Data description: Remotely sensed sea-ice observations

To compare the model output to available observations, we accessed output from two gridded satellite products to calculate: (1) the classic variables using daily 25 km SIC observations from the National Snow and Ice Data Centre (NSIDC, Cavalieri et al., 1996, updated yearly); and (2) climatologies of SIT for July-August and September using monthly SIT derived from Envisat and Cryosat-2 with a 50 km smoothing radius, distributed by the Archiving, Validation and Interpretation of Satellite Oceanographic (AVISO) data portal (Guerreiro et al., 2017). The AVISO product is available from 2003 and comprises 3 different sampling

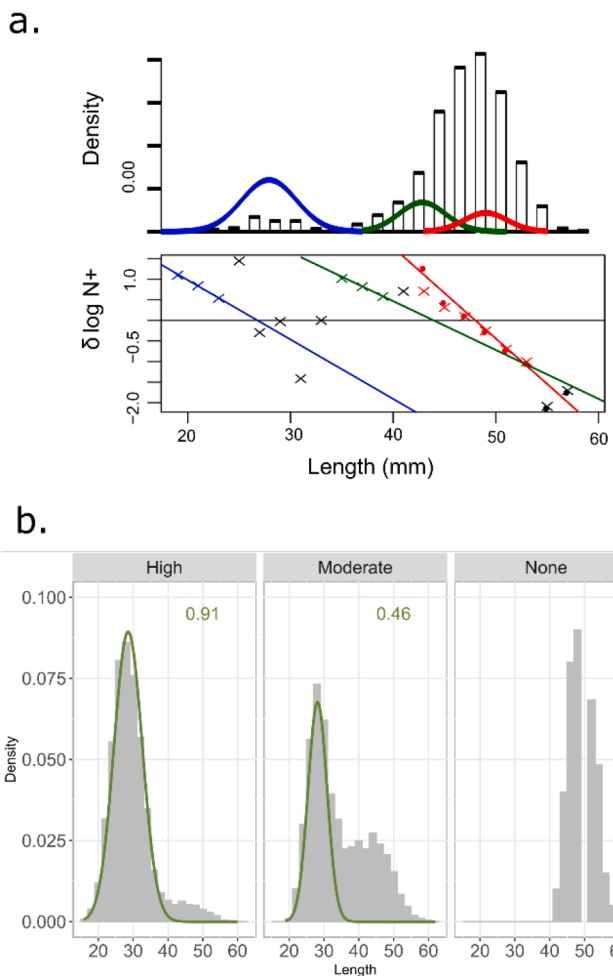


Fig. 2. The derivation of R_1 from length frequency data. This method involved using a. the Bhattacharya method to inform b. a Gaussian mixture analysis. In a. an example of the Bhattacharya method mixture analysis is shown for the Bransfield region in 1994. The upper bar graph refers to the length-frequency distribution. The lower plot shows the sample calculation. Here the log of the data can be approximated by a parabola, which can be further simplified to a straight line by differencing. Thus, by plotting the logarithmic difference of each length frequency class against its midpoint, separate components can be identified by drawing straight lines through the data, as shown. In b., varying resulting R_1 values (for cases where high, moderate and zero R_1 values were calculated), are drawn in green over their original length-frequency distributions (S. Georgia E. in 1982, Bransfield in 1982 and Weddell N.E. in 2009 are shown as examples from left to right). (For interpretation of the references to colour in this figure legend, the reader is referred to the web version of this article.)

methods (Fig. C.3). Where overlap between two sampling methods occurred, the most recent was used.

2.3.3. Evaluating model against observations

As an additional verification, we performed evaluations comparing modelled output of sea-ice variables with available satellite products. These included an evaluation of modelled SIC and the marginal ice zone (MIZ). The latter is important for our study, as previous work had hypothesized the importance of the MIZ for krill habitat (Meyer et al., 2017), and our choice of modern variables reflects this (Table 2). It is therefore crucial that the model represent the MIZ reasonably. A sensitivity analysis (Appendix C.i) enabled us to provide a realistic MIZ representation in terms of area and location (Fig. 3). The model's representation of SIT was also evaluated against remotely sensed SIT (Appendix C.ii), which revealed that the model represented spatial patterns

of SIT well. Although modelled SIT was lower than observed, it was close to the lower confidence limit of observed SIT and therefore within a reasonable range. Additionally, inter-instrument differences in the Antarctic are large (Fig. 3 in Kacimi and Kwok, 2020), giving relatively low confidence in the remotely-sensed product.

2.3.4. Modern variables: Achieved through model output

We developed a suite of modelled sea-ice variables providing a more mechanistic description of krill sea-ice habitat: we term these “modern” variables. These variables are available through use of sea-ice models, and/or reflect new perceptions of krill overwintering habitat.

Recent work suggests that SIC, SIT and RR are likely important for describing larval habitat (Meiners et al., 2012; Melbourne-Thomas et al., 2016; Meyer et al., 2017). In particular, the distribution of these variables was identified as important (Meyer et al., 2017). To characterize the distribution of SIC, SIT and RR, the daily model output for each was summarized into modern variables using the summary statistics. The summary statistics used included mean, standard deviation (sd) and coefficient of variation (cv, sd/mean) for all sea-ice variables, as well as the percentage of time (days) that a cell was classified as MIZ (% MIZ cover). Both the maximum RR and the mean-mode (*i.e.* mean minus mode) SIT were used as proxies for sea-ice deformation (*i.e.* under-ice habitat structural complexity). Previous work also hypothesizes that krill may alter their use of sea-ice habitat depending on the stage of the season (Meyer, 2012), so we summarised the daily model outputs for midwinter (Jul-Aug) and late winter (Sep) separately.

2.4. Correlations between recruitment and sea ice variables

To identify sea-ice drivers of krill recruitment, maps of temporal correlations were calculated between recruitment indices in key regions and the suite of modern sea-ice variables. Of these initial modern variables, five had the strongest magnitude and spatial area of correlations and also had support from literature (Table 2). We therefore focussed the analysis on these five. Using estimated sea-ice variables from the model brought new structure and definition to overwintering habitat composition (Fig. C.5-6). For comparison, correlations to the classic sea-ice variables (DUR, TOA and TOR) were also calculated.

Maps of temporal correlations were generated by calculating the Pearson's correlation between the time series of sea-ice variables within every model grid cell over the entire study area and the time series of log recruit density (excluding zero values) per hexagonal region. This resulted in a map of temporal correlation that had the same grid as the model. Zero values of log recruit density were excluded to avoid zero-inflation and over dispersion that would be caused by a high occurrence of seasons with an R_1 (and thus recruit density) of zero. This raises the question of whether these zeros are “real” (*i.e.* does failing to sample a small size class truly reflect zero recruitment). It is more likely that these size classes were present but were not sampled. This issue requires a more in-depth analysis into how recruitment is inferred from length frequency data and is beyond the scope of this paper.

As an indicator of which correlations are unlikely to have arisen by chance, we performed a permutation test. This involved iteratively shuffling the ordering of the recruitment time series and recalculating the map of temporal correlation to generate a frequency distribution of correlations that would result from the randomized data. This provides a random distribution of correlations against which to compare our observed correlations. If the observed correlations occur at the tail ends of the permuted distribution, they are more likely to be real. The permutation test was performed 100 times for each sea-ice variable and recruitment region. We acknowledge that spatial autocorrelation and multiple testing may increase the chance of a type I error in spatial maps of temporal correlation and permutations. Therefore, we also summarized permuted maps (which have the dimensions of the model grid) using two whole-of-area statistics: the mean of the absolute correlation for all the model grid cells, and the 95% quantile. Since these

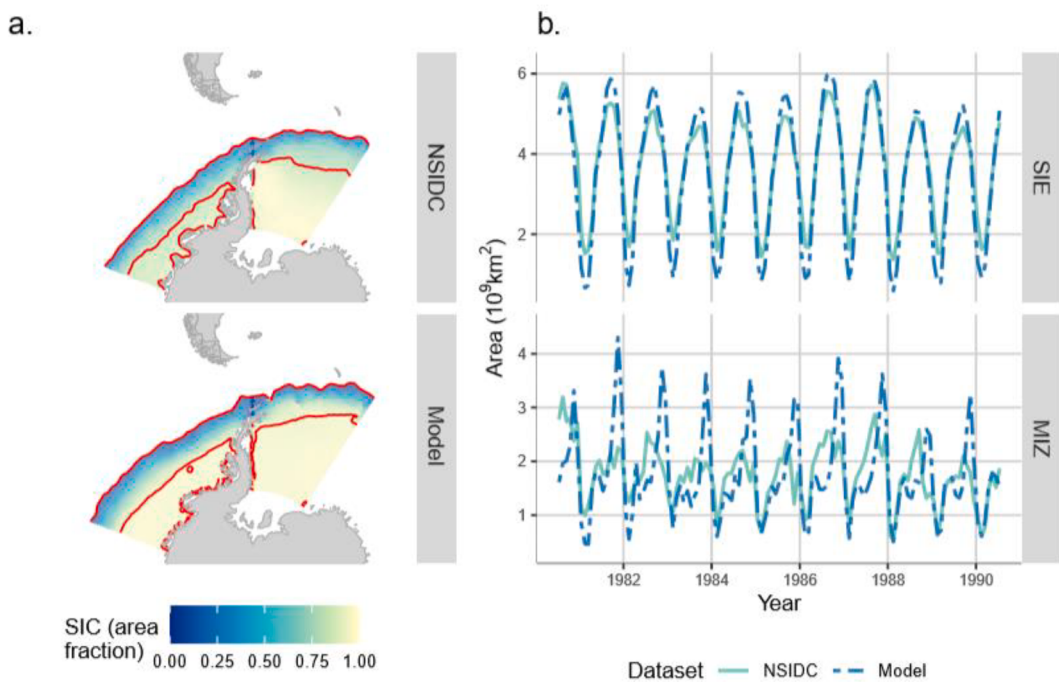


Fig. 3. Validating COCO the modelled SIE and MIZ against NSIDC observations. Panel a. displays the similarity in SIE and MIZ location, showing SIC between NSIDC and COCO the model for September, averaged over 1979–2016. Red contours outline the MIZ along the 0.15 and 0.80 ice concentration fraction isolines in NSIDC, and the 0.9 < DO YOU MEAN 0.09? 0.9 doesn't make sense!> and 0.92 isolines in COCOthe model. Panel b. validates how well COCO the model can reproduce interannual variation in SIE and MIZ area, using a monthly timeseries of SIE and MIZ area. (For interpretation of the references to colour in this figure legend, the reader is referred to the web version of this article.)

summarized statistics required considerably less data storage, we were able to run 500 permutations for the whole-of-area statistics.

2.5. Larval transport

Finally, to provide context for the spatial correlations resulting from the above analysis and evaluate the prospect of remote connections, we also considered larval transport.

2.5.1. Data description: Sea-ice and surface current velocities

Sea-ice velocity fields were used to calculate back-trajectories of krill transport when sea ice was present. Previous analyses (e.g. Meyer et al., 2017; Thorpe et al., 2007) have used the Polar Pathfinder daily 25 km resolution EASE-Grid sea-ice velocity vectors from the National Snow and Ice Data Center (NSIDC) (Tschudi et al., 2019). However recent evaluations of NSIDC velocities against buoy data have found measurement artefacts that can significantly affect analysis results (Szanyi et al., 2016), as well as an underestimation of ice velocity (Sumata et al., 2014). We therefore used sea-ice velocities calculated from the satellite microwave sensors AMSR-E and AMSR-II images using a method based on maximum cross correlation (Kimura and Wakatsuchi, 2011). This “Kimura” dataset is structured on a 60 km resolution grid in daily timesteps from 2003 to 2016. The Kimura dataset has reproduced sea-ice velocities in the Arctic with a high degree of accuracy when validated against buoy data (Kimura et al., 2013), although such a validation has yet to be done in the Southern Ocean.

The ocean surface current velocity fields were produced by SSALTO/DUACS and represent altimetry-derived dynamic topography heights and geostrophic velocities. This provides a measure of the mesoscale geostrophic component of flow. The product is available on a 1/4° grid in daily timesteps from 1993.

2.5.2. Particle tracking

To determine likely transport pathways, 15–20 (depending on the area covered by ocean) equally spaced points were laid in each

recruitment region. For each of these points Lagrangian back-trajectories over the winter months were calculated from November 30th to April 1st of the same year (Meyer et al., 2017), following the method of Tison et al. (2020). This was done for every year from 2003 to 2016. The trajectories were updated in 12 h timesteps. When sea-ice velocity data was present, one timestep (12 h) of the day was advected with sea ice, and a second timestep was advected with under-ice surface currents. Since sea-ice cover inhibits the remote measurement of under-ice surface currents, they were estimated by scaling the magnitude of the altimetry-derived sea-ice velocity components by 0.43 and applying an offset of -35 to the direction (Meyer et al., 2017). When sea-ice velocity data was absent, the particle was advected with surface currents for both timesteps. The position of the particle was recorded every 10th day of the simulation to thin the data. For more detail on the particle tracking method, see Appendix E.

All analyses were performed in the R statistical computing environment (R Core Team, 2018). For packages used see Table A.1.

3. Results

3.1. Krill recruit density

The krill data were processed to provide time series of mean krill density and pooled length frequency for nine polygons, termed “recruitment regions” (green hexagons in Fig. 1). Overall, these time series spanned from 1981 to 2016, but the sampling coverages available from the krill density and length-frequency databases varied by recruitment region (Tables B.1–2). Thus, these data supported calculations of proportional recruitment, krill density, and recruit density with variable temporal coverage (Fig. 4, Tables B.3–5).

The interannual trend in log₁₀-transformed recruit density calculated across our nine recruitment regions ($-0.046 \log_{10}(\text{recruit density no/m}^2)/\text{year}$, $\text{Pr}>|t|=8.87 \times 10^{-3}$, adjusted $R^2=0.11$, see Fig. B.1) was similar to a previously published trend calculated from data pooled across the southwest Atlantic (-0.070 , $P<0.001$, adjusted $R^2=0.39$)

(Atkinson et al., 2019). As to be expected there was more noise around our model fit for regional recruit density. Since our model structure did not explicitly account for region, the variation due to region was unexplained and resulted in a lower adjusted R^2 .

3.2. Linking krill recruitment and sea ice

3.2.1. Correlations with sea ice

Our selection of modern variables revealed spatial distributions in sea-ice characteristics that could not have been identified from sea-ice concentration (SIC) observations alone (Fig. 5). Highlighted regions include the Weddell-Scotia Confluence, the southwestern Weddell Sea, coastal regions, and the ice edge. This allowed us to identify new patterns of correlation with recruit density.

To present the most rigorous findings we focused our results interpretation on those correlations that were most likely to be real, arising from the three best-sampled recruitment regions, as a robust correlation analysis requires a well-populated time series. These regions were: wAP mid., Bransfield and S. Georgia E. (Figs. 1 and 4); the full correlation maps from the six lesser sampled recruitment regions are provided in Fig. D.1. To determine correlations unlikely to have arisen by chance the maps of temporal correlations were interpreted alongside the permutation results (mapped in Fig. D.2, summarised by whole-of-area statistics in Fig. D.3).

Maps of the temporal correlations and permutations revealed distinct, large areas where these sea-ice indicators correlated with

regional recruit densities (Fig. 6, Fig. D.4-5). These areas were often not located in the same region from which the recruit density was derived, thus we termed these areas “remote connections”. Collated at the whole-of-area scale, permutation results indicated six cases where the modern sea-ice variables are very likely to provide real correlations with our regional-scale recruitment densities (Fig. D.3). These include wAP mid. recruitment correlating with Jul-Aug mean-mode sea-ice thickness (SIT), Jul-Aug maximum (max) ridging rate (RR) and Sep standard deviation (sd) of ridging rate (RR); Bransfield recruitment correlating with Sep marginal ice zone (MIZ) coverage; and S. Georgia E. recruitment correlating with Jul-Aug max RR and Sep MIZ coverage. Therefore, we are most confident in the maps of correlations and permutations that correspond to these particular sea-ice indicators. However these whole-of-area statistics can dilute signals from even fairly large-scale features which the permutation maps indicate to very likely be real (e.g. influence of Sep MIZ coverage for Bransfield recruitment, Figs. D.2 & D.4); their spatial size and coherence indicates a non-random phenomenon, so we have reasonable confidence to focus our presentation of remote connection results to the larger-scale features for our three best-sampled recruitment cells.

Among the classic variables (Fig. 6), we found good correspondence between the correlation maps produced by the NSIDC and model datasets, indicating that the model could effectively reproduce the spatio-temporal dynamics of SIC suitable for our study. Remote connections for the classic variables were generally small in area. In the cases of the wAP mid. and Bransfield regions, positive correlations extended eastward

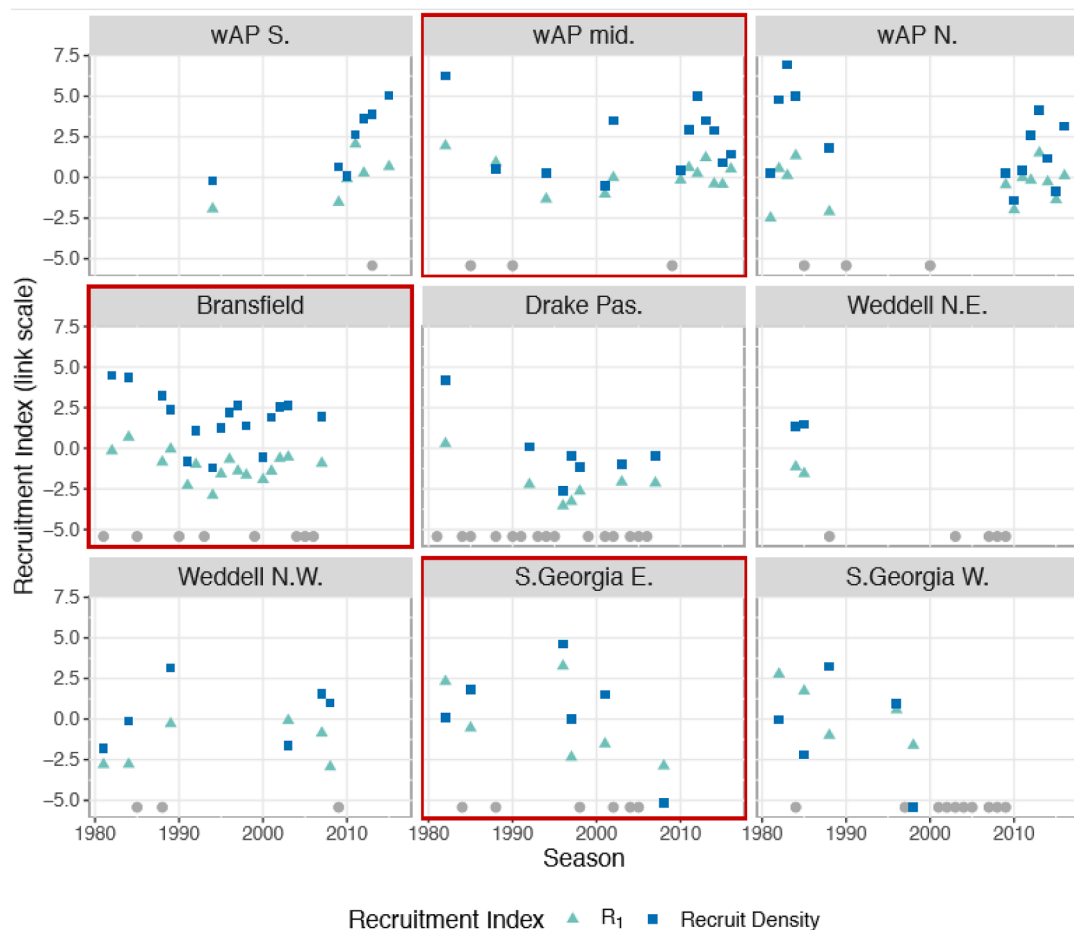


Fig. 4. Derived regional-scale time series of krill recruitment indices. R_1 (proportion of 1-year-old krill in the population, green triangle) and recruit density (blue square) are plotted on their relevant link scale (i.e. logit-link for R_1 and log-link for recruit density). Note the two indices are related as recruit density is R_1 weighted by the mean standardized krill density for that region and season. Seasons where sampling occurred but recruit density was zero are indicated by grey circles at the bottom of the graph. The sea ice correlation analysis focused on three of the best-sampled recruitment regions (outlined in red). (For interpretation of the references to colour in this figure legend, the reader is referred to the web version of this article.)

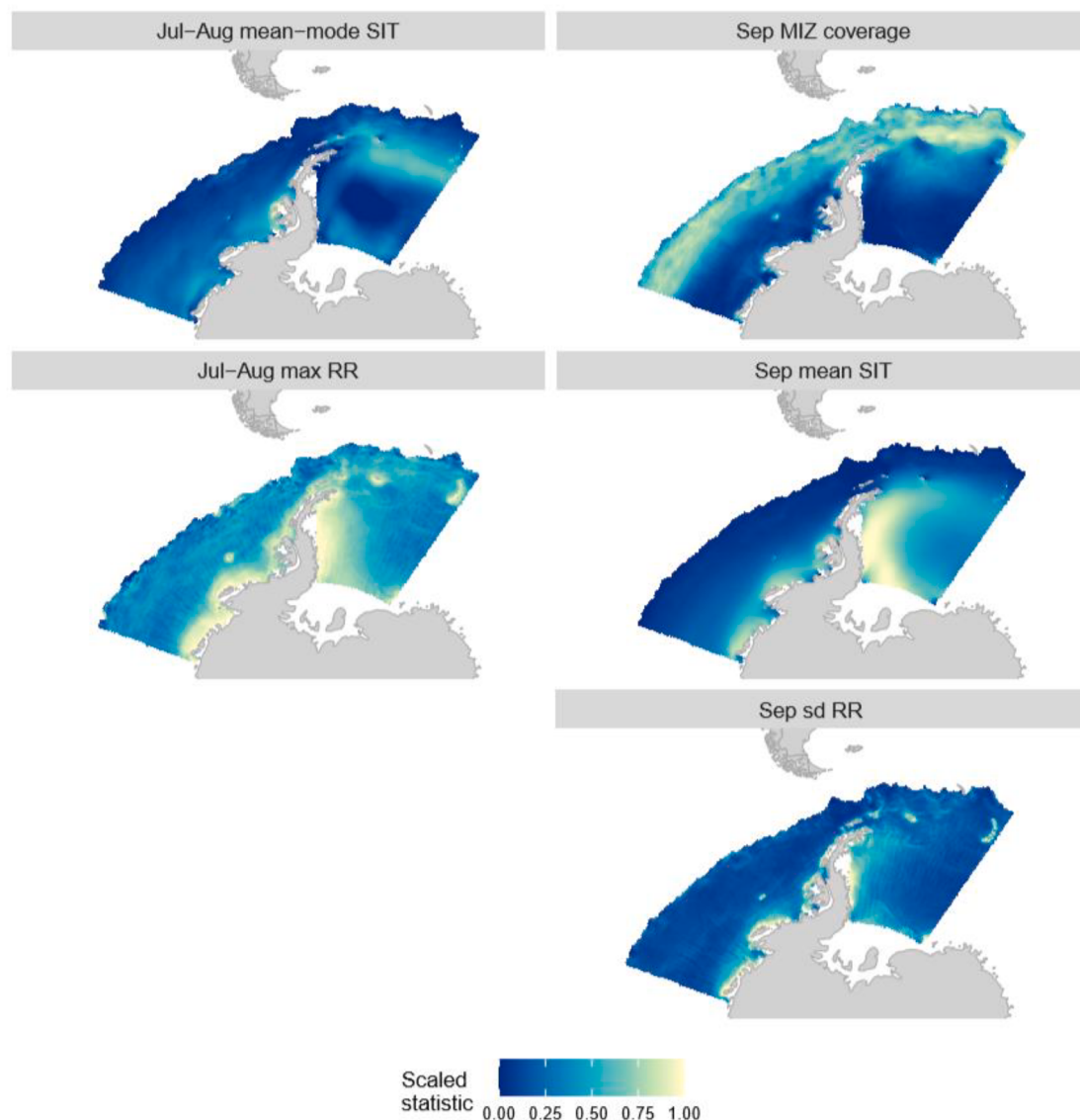


Fig. 5. Climatologies of key sea-ice habitat variables. These climatologies represent spatial averages of their respective variables, calculated from the model output from 1979 to 2016. For example, the map for Jul-Aug max RR represents an average of the maximum RR that occurred over July and August for each year. Each variable has been scaled from 0 to 1 so that they can be plotted on the same colour scale. Both Jul-Aug max RR and Sep sd RR maps have been capped at their 95% quantiles; this was done so that extremely high values near the coast would not mask the structuring of RR values further offshore.

(downstream), while negative correlations extended westward along the MIZ in the Bellingshausen and Amundsen Seas as well as occurring in the southwest corner of the Weddell Sea. For S. Georgia E. the remote connections were mostly positive and more dispersed, extending westward from the Bransfield Strait and throughout part of the Weddell Sea.

Remote connections identified using the modern modelled variables generally encompassed a larger area and highlighted different regions than the classic variables. For the wAP mid. these included a region of positive correlation spanning the Bellingshausen/Amundsen Seas, a positive correlation along the eastern peninsula (western Weddell Sea) and a negative correlation reflected in the greater Weddell Sea. A relatively similar pattern was evident in the west (positive) and east (negative) of the study domain for the Bransfield region. S. Georgia E. showed strong negative correlations with sea ice in the western and southern areas of the Weddell Sea. In addition, a thin arc of positive correlation occurred along the northern ice edge extending westward (upstream) from S. Georgia along the South Scotia Ridge. While this appears to be a series of smaller elements, a holistic look at the surrounding correlations reveals it is part of a larger ice-edge feature which

spans all three modern sea-ice variables for September (*i.e.*, MIZ coverage, mean SIT and sd RR; Fig. D.4). Albeit with less confidence, the continuity and spatial area suggest that it may indeed represent a real physical habitat feature.

Finding remote connections with sea ice supports the theory that krill may associate with and be transported by sea ice. An exploration of sea-ice back trajectories is therefore needed to determine whether this explanation for the remote connection is likely, and if so, which remote connections are likely to have mechanistic drivers.

3.2.2. Larval transport

The larval transport analysis allows for the remote connections observed in the correlations to be interpreted through a mechanistic lens (Figs. 7 & E.1). These results indicate that recruitment in the wAP mid region may be, in part, driven by larval transport with sea ice from the Bellingshausen Sea. Similar inferences can be drawn between recruitment in the Bransfield region and sea ice in the western Weddell Sea, as well as South Georgia and sea ice along the northern ice edge of the Scotia Sea.

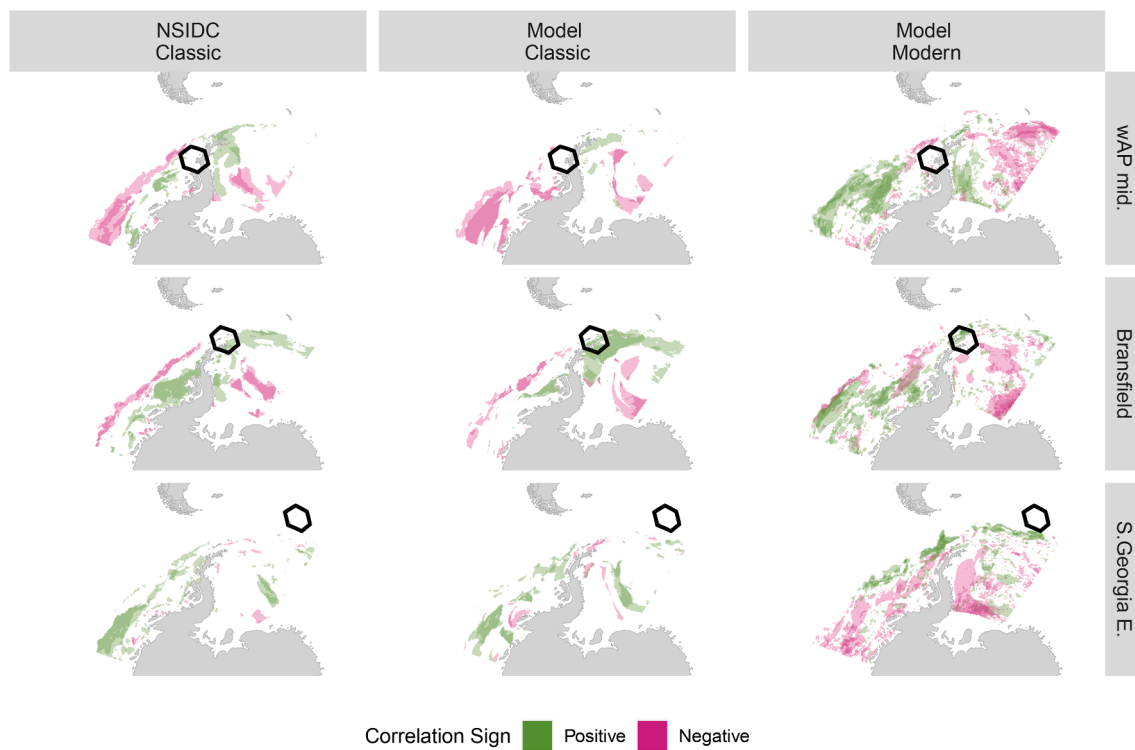


Fig. 6. New regions of high correlation between recruit density in main cells and modern sea ice variables. These maps compare correlations to (columns left to right): classic variables (DUR, TOA, TOR) calculated using NSIDC SIC observations; classic variables calculated using the modelled SIC output; the modern sea ice variables identified using the model (Table 2). Note that this therefore compares the overlay of 3 variables for the two left columns, and 5 variables for the right column. Coloured regions show where the observed correlation was at the tail ends of the permuted distribution, to the 10% level. For TOA, the sign of the correlations is reversed, as an earlier (*i.e.* smaller) TOA results in longer DUR. Correlations for each of the variables are overlaid with transparency, so each map represents a composite of the positive and negative correlations generated from each set of variables. Correlations are displayed for the three best-sampled recruitment regions. For maps that separate these high correlation areas into their component variables, see Fig. D.4-5.

4. Discussion

The temporal correlations between regional recruit density and sea ice reveal remote connections which vary by recruitment region. These remote connections are often driven by multiple spatially overlapping sea-ice variables, but differ substantially depending on whether the sea-ice variables used were classic descriptors of sea-ice habitat (derived from observed SIC) or the modern variables (derived from sea-ice model output) developed within this study. Assuming the sea-ice variables represent real functional relationships between larvae and sea ice, then the remote connections should follow overwinter transport pathways from source regions to each recruitment region. We find that the remote connections derived from our modern sea-ice variables correspond well with overwinter larval transport, adding value to existing classic sea-ice variables in defining overwinter habitat quality.

In S. Georgia E., recruitment studies generally conclude that the population is not self-sustaining, and that recruits are transported from elsewhere (Siegel and Watkins, 2016). Current understanding of krill transport to South Georgia supports the remote connections we found for S. Georgia E.. Transport studies have identified source populations for South Georgia, finding krill advected from the north-western Weddell Sea by the Weddell Gyre or Weddell-Scotia Confluence, and from the wAP by the Antarctic Circumpolar Current (ACC) (Fach and Klinck, 2006; Hofmann et al., 1998; Mackintosh, 1972; Marr, 1962; Meyer et al., 2017; Murphy et al., 2004). The remote connections identified with classic variables tended to be smaller in area, but the identification of regions near the ice edge in the Bransfield Strait supports earlier findings that changes in SIE and timing may interact with ocean circulation to affect krill transport to South Georgia (Murphy et al., 2004, 1998; Thorpe et al., 2007). Remote connections with the modern variables

were more extensive and displayed a more connected network of possible transport pathways. Most notable was the strong negative correlation in the western and southern Weddell Sea. This was driven mainly by July-August maximum (max) ridging rate (RR) and September mean sea-ice thickness (SIT), indicating that lower values of these variables are related to higher recruitment in South Georgia (Fig. D.4). A lower RR and SIT could indicate that the ice is diverging, which would be linked to higher export by the Weddell Gyre to South Georgia. This remote connection matches where krill likely originate in the Weddell Sea, assuming they arrive in the productive marginal ice zone (MIZ) along the South Scotia Ridge by mid-September (Meyer et al., 2017). Krill would then be capable of reaching South Georgia by December (~76–89 days, Murphy et al., 2004). Larval back-trajectories support these previously studied transport pathways, reinforcing the importance of the South Scotia Ridge.

Furthermore, we found a semi-continuous arc of high positive correlation along the South Scotia Ridge with S. Georgia E. recruitment. This may coincide with the eastward drift of the northern ice edge, transported by the ACC through the Drake Passage and across the Scotia Sea towards South Georgia. This is a well-evidenced transport route for krill to South Georgia (Fach and Klinck, 2006; Hofmann et al., 1998; Murphy et al., 2004, 1998; Thorpe et al., 2004). It is feasible that krill arriving in South Georgia by spring-summer are found along this route in mid-late winter. This remote connection also coincides with the MIZ and is evident within all our modern September sea-ice variables, which is when we expect the MIZ to be most important for krill recruitment. By providing a food-rich environment, transport associated with the MIZ may explain the larger krill lengths observed in South Georgia compared to upstream source regions (Fach et al., 2002; Siegel and Watkins, 2016). We also note this feature extends past the tip of the Antarctic Peninsula

(AP), which includes key krill habitat in the South Shetland Islands and Bransfield Strait. Particle tracking using ocean transport has shown January krill may have come from as far as the South Shetland Islands in October (Murphy et al., 2004). Another study using velocities from surface drifting buoys suggested a transport time of 110 days, placing krill at the South Shetlands by mid-September (Ichii and Naganobu, 1996). Our larval transport analysis agrees with these transport times (Fig. 7). This region was particularly highlighted by a positive correlation with July-August mean-mode SIT (Fig. D.5). This indicator of sea-ice rugosity may suggest that sea ice in the South Shetland Islands and Bransfield Strait functions as a refuge for krill on their way to South Georgia in early winter. Thus, there may be true mechanistic links driving these feature, despite weaker correlations.

In the western Antarctic Peninsula (wAP), the presence of the AP as a land barrier to the east dictates that incoming krill originate from the west, and sea-ice dynamics within the Amundsen and Bellingshausen Seas regions have been found to be important for explaining krill recruitment variability (Piñones et al., 2013; Wiedenmann et al., 2009). The remote connections we identified using classic variables highlighted negative correlations with sea ice especially in the northern Amundsen Sea, which is inconsistent with existing evidence. They therefore seem less likely to represent plausible sea-ice habitat descriptors for krill recruiting in the wAP mid. The modern variables, however, identified a large remote connection (strong positive correlation) spanning both seas. This was located somewhat farther upstream than hypothesized source regions for the wAP (Piñones et al., 2013), but previous particle tracking studies mainly considered only ocean currents for transport. Our larval transport analysis that incorporates sea ice indicates that the remote connections in the western Bellingshausen Sea are indeed feasible source regions for krill in the wAP mid. If longer transport times or an increased association with sea ice (which moves ~2x faster than surface currents) were to be considered, it is highly likely the Amundsen Sea would also be included. This agrees with studies showing that

considering sea-ice transport can enhance the distance travelled (Meyer et al., 2017; Thorpe et al., 2007). Therefore, recruitment in the wAP mid region may be partially driven by transport through sea ice in the Amundsen and Bellingshausen seas.

The positive remote connection spanning the Amundsen and Bellingshausen seas was supported by the overlap of the three September sea-ice indicators (Fig. D.4). Together, these indicators suggest that thicker, more dynamic sea ice in these areas at the end of winter was most influential for high recruitment in the wAP mid. Such icescapes may result from dynamic processes such as storms that would contribute to sea ice thickening and ridging events. This would create over-raftered sea ice for refuge and more complex feeding substrate (Meyer et al., 2017), as well as potentially release ice algae into the water column (Table 1). Sea ice habitat in the Amundsen and Bellingshausen seas may therefore provide important refuge and increased food availability during late winter for larvae en route to the wAP.

Despite evidence for local origins of krill within the wAP (summarised in Piñones et al., 2013), neither set of variables (classic nor modern) identified high correlations with local sea-ice indicators (Fig D.5). This is possibly due to the shallow bathymetry in continental shelf areas that may provide a food-rich habitat which may facilitate diverse feeding strategies and reduce reliance on sea ice (Schmidt et al., 2014; Walsh et al., 2020). Shallow bathymetry has been assumed to limit successful spawning (Hofmann and Hüsrevoglu, 2003; Thorpe et al., 2019). Our findings may therefore indicate that the environmental conditions that interact to define good habitat within the shelf regions are complex and likely include more than just sea-ice processes.

In the Bransfield region, Lagrangian particle tracking has identified diverse source regions, such as the Bellingshausen and western Weddell seas (Capella et al., 1992). Our larval transport analyses are consistent with this. The remote connections derived from classic and modern variables both highlighted some positive correlations upstream in the Bellingshausen Sea, but in general the correlations for Bransfield

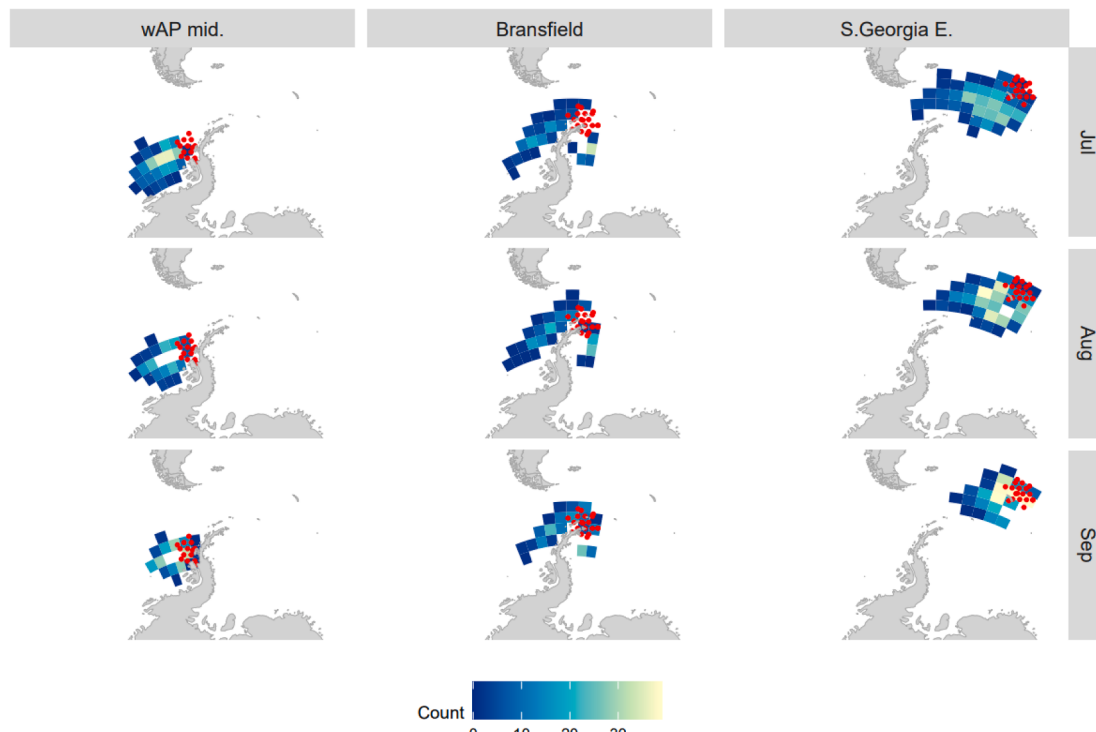


Fig. 7. Monthly distribution of krill source regions using sea-ice transport. Sea ice back-trajectories were calculated from November 30th of each year (2003–2016) at end locations indicated by the red dots. The progressive locations of the particles along the back-trajectories were recorded every 10 days. The resulting locations across all years were binned to a 4×2 degree grid. Grid cell counts represent the number of binned locations along a back-trajectory occurring in a given month (e.g. to show where particles that end up at a given location were in July, etc.). (For interpretation of the references to colour in this figure legend, the reader is referred to the web version of this article.)

recruitment were weaker than those found for wAP mid. or S. Georgia E. (Fig. D.4). Some small negative correlations with September mean SIT and standard deviation (sd) RR in the western Weddell Sea may be linked to increased sea-ice divergence and export of krill into the Bransfield Strait. There were also localized positive correlations around the South Shetland Islands with most sea-ice indicators, particularly September mean SIT (Fig D.5). This could indicate a hotspot of important habitat for larval overwintering around the South Shetland Islands. However, due to the small area of this feature it is difficult to validate this finding from current observations. These less conclusive findings may also reflect the emerging view that krill in this region have flexible overwintering strategies and are less reliant on sea-ice habitats. Alternatively, correlations could be masked by the diverse composition of krill in the Bransfield region, which reflects krill from different source regions and life histories.

In addition to remote connections that have likely mechanistic drivers, we observed two predominant signals of climate modes within the remote connections. First was a dipole of positive correlations to the west of the AP and negative correlations to the east amongst the modern sea-ice variables for both the wAP mid. and Bransfield regions. Using inferences based on larval transport, we can attribute the western positive correlations to likely source regions, as well as correlations in the western Weddell Sea for the Bransfield region. We speculate that the remainder of the remote connections found in the Weddell Sea are likely the result of atmospheric correlations. This dipole invokes the patterns of large-scale atmospheric modes that operate in the area, such as the Pacific-South America mode (Mo and Higgins, 1998), the El Niño Southern Oscillation (ENSO) (Turner, 2004), and zonal wave three (Raphael, 2007). These modes have been shown to have a strong influence on Antarctic sea-ice patterns (Murphy et al., 2014; Yuan and Li, 2008), as well as correlate to larval growth and recruitment (Loeb and Santora, 2015; Massom and Stammerjohn, 2010; Massom et al., 2006).

These climate modes may also play a role in a second climate-related pattern. This pattern was composed of negative remote connections extending westward from the AP along the MIZ and was formed by classic variables for the wAP mid. and Bransfield regions. This pattern is similar to that observed during a sea-ice compaction event. In these events, a quasi-stationary zonal wave three, along with a weak La Niña (in the 2005 event) or a positive Southern Annular Mode (2001/2 events) were associated with atmospheric anomalies that drove persistent north westerly winds (Massom et al., 2008, 2006). The deepening of the Amundsen Sea Low can drive such winds causing extreme ice compaction towards the coast in the Amundsen and Bellingshausen seas (Raphael et al., 2016). Such events resulted in earlier ice retreat (Massom et al., 2008, 2006), which may explain why this signal is resolved by the classic sea-ice variables. Observations indicate that compaction events have negative impacts on larval growth and recruitment (Massom and Stammerjohn, 2010; Massom et al., 2006). We should then expect to see a positive correlation between the ice edge and krill recruitment (shorter ice coverage = lower recruitment) rather than the negative correlation observed. Yet these compaction events can also result in increased ice melt and primary production (Massom et al., 2006), as well as thicker ice and increased ridging near the coast (Massom et al., 2008, 2006), which may create more favourable habitat from a mechanistic perspective. Thus, while these correlations may indicate an indirect mechanistic connection to krill recruitment and an importance of wAP compaction events, their influence on krill recruitment requires further exploration.

5. Conclusions

Overall, the correlations between recruit density and our modern sea-ice variables represent an improved approximation of krill overwinter habitat quality. Early analyses exploring the relationships between krill recruitment and sea ice identified classic sea-ice variables, such as duration, time of arrival, and time of retreat, as important, and

the remote connections resulting from these classic variables corroborate many of these early findings. The remote connections from our modern sea-ice variables improve upon this by using a more mechanistic description of the sea-ice habitat to identify more probable source regions and more extensive and connected networks of transport pathways. These include source regions for South Georgia in the western and southern Weddell Sea as well as transport pathways along the South Scotia Ridge; source regions for the wAP in the Amundsen and Bellingshausen seas; and source regions for the Bransfield region in the Bellingshausen and western Weddell seas. These results provide a step-change forward from exploring correlations between recruitment and environmental parameters to an understanding of the mechanisms that lead to these correlations.

Our results have important implications in progressing current paradigms of how krill are responding to climate change. Our results support the emerging view that the impact of changing sea-ice dynamics on krill recruitment is nuanced (Melbourne-Thomas et al., 2016; Meyer et al., 2017; Saba et al., 2014). It is likely that krill respond to changes in sea ice quality, bounded by changes in sea-ice extent and timing. Furthermore, regional variation in dependencies on sea ice, e.g., evidenced by a lack of strong remote connections in the Bransfield region, may provide pockets of resilience to climate-driven changes in sea-ice dynamics.

To robustly quantify the impacts of climate change on krill populations, progression beyond correlations to statistical models with mechanistic underpinnings is needed (Murphy et al., 2018; Quetin et al., 2007). Ideally, the most robust assessment method would be to develop a model that simulates the krill life cycle and population dynamics in response to environmental drivers, so that spatial estimates of krill biomass could be achieved. Currently, a lack of quantification in how changes in sea ice quality impact recruitment serves as a main barrier to simulating krill population dynamics. This has been hindered by uncertainties in measuring krill recruitment, as well as limited spatio-temporal coverage in measurements of sea ice physical-biological properties (Meiners et al., 2017).

Our study begins to address this important knowledge gap. We identify a new suite of sea-ice variables that improve understanding of the relationship between sea ice and krill. These variables explicitly describe the physical habitat properties of sea ice, while considering its biological properties indirectly. Here our choice of sea-ice model is informed by our aims to compliment emerging satellite products, such as sea-ice thickness and rugosity (Tamura et al., 2015; Toyota et al., 2011), as well as snow thickness and under-ice currents. In the future, exploring the biological properties of sea ice explicitly will be vital to further quantifying these promising relationships. This could involve a model that represents sea ice biology, alongside mesoscale in-situ measurements of sea-ice variables related to food availability (e.g. Castellani et al., 2020). Future analyses may also account for the effects of varying larval overwinter back-trajectories. Variations in transport would result in different life histories of exposure to sea ice habitats (Kohlbach et al., 2017), therefore integrating our sea-ice indicators along back-trajectories will give further insight into the effects of varying life histories on larval condition and recruitment.

CRediT authorship contribution statement

Devi Veytia: Conceptualization, Data curation, Formal analysis, Investigation, Methodology, Visualization, Writing - original draft, Writing - review & editing.

Author contributions

All authors contributed to conceptualization, methodology, formal analysis and writing. S.C., S.B., S.K., K.M. and E.M. contributed to the supervision of D.V.

Declaration of Competing Interest

The authors declare that they have no known competing financial interests or personal relationships that could have appeared to influence the work reported in this paper.

Acknowledgements

The authors acknowledge the contributions of all the data providers of the krill density and length frequency data. D.V. is the recipient of a Tasmania Graduate Research Scholarship provided by the University of Tasmania. S.B. is the recipient of an Australian Research Council Australian Discovery Early Career Award [project DE180100828]. E.M. was supported by the BAS ALI-Science Ecosystems project (developing krill life-cycle models and future projections) and acknowledges BAS colleagues for discussions on the development of analyses, models and projections of Antarctic krill population processes. S. Wotherspoon provided very helpful guidance regarding the permutation analyses. This research was supported by the Australian Government [Antarctic Science Projects 4408 and 4512], and through the Antarctic Science Collaboration Initiative program as part of the Australian Antarctic Program Partnership. The study is also a contribution to the international Integrating Climate and Ecosystems Dynamics Programme (ICED). K. K. was supported by JSPS KEKENHI [grants JP19K12301 and JP17H06323]. The surface velocity data were produced by SSALTO/DUACS and distributed by Aviso+, with support from Cnes (<http://www.aviso.altimetry.fr/duacs/>). The altimetry sea ice thickness data used in this study (doi 10.6096/CTOH_SEAICE_2019_12) were developed, validated by the CTOH/LEGOS, France and distributed by Aviso +.

Data statement

KRILLBASE density data are freely available (<https://www.bas.ac.uk/project/krillbase/>). KRILLBASE length frequency data are available from the British Antarctic Survey by request (contact: Simeon Hill, sih@bas.ac.uk), and the Palmer LTER length frequency data are available online (<https://doi.org/10.6073/pasta/be42bb841e696b7bcad9957aed33db5e>). Ocean-sea ice model output are available from K.K. upon request (kazuya.kusahara@gmail.com). For sea-ice velocity fields from the Kimura dataset, contact N.K. (kimura_n@aori.u-tokyo.ac.jp). The remotely-sensed surface velocity and sea-ice thickness products are available on Aviso+ (<http://www.aviso.altimetry.fr/>).

Appendix A. Supplementary data

Supplementary data to this article can be found online at <https://doi.org/10.1016/j.ecolind.2021.107934>.

References

- Arrigo, K.R., 2014. Sea ice ecosystems. *Ann. Rev. Mar. Sci.* 6, 439–467.
- Arrigo, K.R., Thomas, D.N., 2004. Large scale importance of sea ice biology in the Southern Ocean. *Antarct. Sci.* 16, 471.
- Arrigo, K.R., Worthen, D.L., Lizotte, M.P., Dixon, P., Dieckmann, G., 1997. Primary production in Antarctic sea ice. *Science* 276, 394–397.
- Atkinson, A., Hill, S.L., Pakhomov, E.A., Anadon, R., Chiba, S., Daly, K.L., Downie, R., Fretwell, P.T., Gerrish, L., Hosie, G.W., 2017. KRILLBASE: a circumpolar database of Antarctic krill and salp numerical densities, 1926–2016.
- Atkinson, A., Hill, S.L., Pakhomov, E.A., Siegel, V., Reiss, C.S., Loeb, V.J., Steinberg, D.K., Schmidt, K., Tarling, G.A., Gerrish, L., Sailley, S.F., 2019. Krill (*Euphausia superba*) distribution contracts southward during rapid regional warming. *Nat. Clim. Change* 9, 142–147.
- Atkinson, A., Siegel, V., Pakhomov, E., Jessopp, M., Loeb, V., 2009. A re-appraisal of the total biomass and annual production of Antarctic krill. *Deep Sea Res. Part I* 56, 727–740.
- Atkinson, A., Siegel, V., Pakhomov, E., Rothery, P., 2004. Long-term decline in krill stock and increase in salps within the Southern Ocean. *Nature* 432, 100–103.
- Bhattacharya, C., 1967. A simple method of resolution of a distribution into Gaussian components. *Biometrics* 115–135.
- Boyd, P.W., 2002. Environmental factors controlling phytoplankton processes in the Southern Ocean. *J. Phycol.* 38, 844–861.
- Brierley, A.S., Fernandes, P.G., Brandon, M.A., Armstrong, F., Millard, N.W., McPhail, S. D., Stevenson, P., Pebody, M., Perrett, J., Squires, M., 2002. Antarctic krill under sea ice: elevated abundance in a narrow band just south of ice edge. *Science* 295, 1890–1892.
- Capella, J.E., Quetin, L.B., Hofmann, E.E., Ross, R.M., 1992. Models of the early life history of *Euphausia superba*—Part II. Lagrangian calculations. *Deep Sea Res. Part I Oceanogr. Res. Pap.* 39, 1201–1220.
- Castellani, G., Schaafsma, F.L., Arndt, S., Lange, B.A., Peek, I., Ehrlich, J., David, C., Ricker, R., Krumpen, T., Hendricks, S., 2020. Large-scale variability of physical and biological sea-ice properties in polar oceans. *Front. Mar. Sci.* 7, 536.
- Cavalieri, D.J., Parkinson, C.L., Gloersen, P., Zwally, H.J., 1996. updated yearly. Sea Ice Concentrations from Nimbus-7 SMMR and DMSP SSM/I-SSMIS Passive Microwave Data, Version 1. NASA National Snow and Ice Data Center Distributed Active Archive Center, Boulder, Colorado USA.
- Cavan, E.L., Belcher, A., Atkinson, A., Hill, S.L., Kawaguchi, S., McCormack, S., Meyer, B., Nicol, S., Ratnarajah, L., Schmidt, K., Steinberg, D.K., Tarling, G.A., Boyd, P.W., 2019. The importance of Antarctic krill in biogeochemical cycles. *Nat. Commun.* 10, 4742.
- Cavanagh, R.D., Murphy, E.J., Bracegirdle, T.J., Turner, J., Knowland, C.A., Corney, S.P., Smith Jr, W.O., Waluda, C.M., Johnston, N.M., Bellaby, R.G., 2017. A synergistic approach for evaluating climate model output for ecological applications. *Front. Mar. Sci.* 4, 308.
- Cox, M.J., Candy, S., de la Mare, W.K., Nicol, S., Kawaguchi, S., Gales, N., 2018. No evidence for a decline in the density of Antarctic krill *Euphausia superba* Dana, 1850, in the Southwest Atlantic sector between 1976 and 2016. *J. Crust. Biol.* 38, 656–661.
- Croxall, J.P., Reid, K., Prince, P.A., 1999. Diet, provisioning and productivity responses of marine predators to differences in availability of Antarctic krill. *Mar. Ecol. Prog. Ser.* 177, 115–131.
- Daly, K.L., 1990. Overwintering development, growth, and feeding of larval *Euphausia superba* in the Antarctic marginal ice zone. *Limnol. Oceanogr.* 35, 1564–1576.
- Daly, K.L., 2004. Overwintering growth and development of larval *Euphausia superba*: an interannual comparison under varying environmental conditions west of the Antarctic Peninsula. *Deep Sea Res. Part II* 51, 2139–2168.
- David, C., Lange, B., Krumpen, T., Schaafsma, F., van Franeker, J.A., Flores, H., 2016. Under-ice distribution of polar cod *Boreogadus saida* in the central Arctic Ocean and their association with sea-ice habitat properties. *Polar Biol.* 39, 981–994.
- De la Mare, W., 1994. Estimating krill recruitment and its variability. *CCAMLR Sci.* 1, 55–69.
- Dee, D.P., Uppala, S.M., Simmons, A., Berrisford, P., Poli, P., Kobayashi, S., Andrae, U., Balmaseda, M., Balsamo, G., Bauer, D.P., 2011. The ERA-Interim reanalysis: Configuration and performance of the data assimilation system. *Q. J. R. Meteorol. Soc.* 137, 553–597.
- Fach, B.A., Hofmann, E.E., Murphy, E.J., 2002. Modeling studies of Antarctic krill *Euphausia superba* survival during transport across the Scotia Sea. *Mar. Ecol. Prog. Ser.* 231, 187–203.
- Fach, B.A., Klinck, J.M., 2006. Transport of Antarctic krill (*Euphausia superba*) across the Scotia Sea. Part I: circulation and particle tracking simulations. *Deep Sea Res. Part I* 53, 987–1010.
- Flores, H., Van Franeker, J.A., Siegel, V., Haraldsson, M., Strass, V., Meesters, E.H., Bathmann, U., Wolff, W.J., 2012. The association of Antarctic krill *Euphausia superba* with the under-ice habitat. *PLoS ONE* 7, e31775.
- Guerreiro, K., Fleury, S., Zakharova, E., Kouraev, A., Rémy, P., Maisongrande, P., 2017. Comparison of CryoSat-2 and ENVISAT radar freeboard over Arctic sea ice: toward an improved Envisat freeboard retrieval. *The Cryosphere* 11, 2059–2073.
- Haas, C., 2004. Late-summer sea ice thickness variability in the Arctic Transpolar Drift 1991–2001 derived from ground-based electromagnetic sounding. *Geophys. Res. Lett.* p. 31.
- Hamner, W., Hamner, P., Obst, B., Carleton, J., 1989. Field observations on the ontogeny of schooling of *Euphausia superba* furciliae and its relationship to ice in Antarctic waters. *Limnol. Oceanogr.* 34, 451–456.
- Hasumi, H., 2006. CCSR Ocean Component Model (COCO) version 4.0. CCSR Report 25. University of Tokyo.
- Hofmann, E.E., Hüsrevoglu, Y.S., 2003. A circumpolar modeling study of habitat control of Antarctic krill (*Euphausia superba*) reproductive success. *Deep Sea Res. Part II* 50, 3121–3142.
- Hofmann, E.E., Klinck, J.M., Locarnini, R.A., Fach, B., Murphy, E., 1998. Krill transport in the Scotia Sea and environs. *Antarct. Sci.* 10, 406–415.
- Ichii, T., Naganobu, M., 1996. Surface water circulation in krill fishing areas near the South Shetland Islands. *CCAMLR Sci.* 3, 125–136.
- Jeffery, N., Maltrud, M.E., Hunke, E.C., Wang, S., Wolfe, J., Turner, A.K., Burrows, S.M., Shi, X., Lipscomb, W.H., Maslowski, W., 2020. Investigating controls on sea ice algal production using E3SMv1. 1-BGC. *Annals of Glaciology*, 1–22.
- Jia, Z., Swadling, K.M., Meiners, K.M., Kawaguchi, S., Virtue, P., 2016. The zooplankton food web under East Antarctic pack ice – A stable isotope study. *Deep Sea Res. Part II* 131, 189–202.
- Ju, S.-J., Harvey, H.R., 2004. Lipids as markers of nutritional condition and diet in the Antarctic krill *Euphausia superba* and *Euphausia crystallorophias* during austral winter. *Deep Sea Res. Part II* 51, 2199–2214.
- Kacimi, S., Kwok, R., 2020. The Antarctic sea ice cover from ICESat-2 and CryoSat-2: freeboard, snow depth, and ice thickness. *The Cryosphere* 14, 4453–4474.
- Kawaguchi, S., Satake, M., 1994. Relationship between recruitment of the Antarctic krill and the degree of ice cover near the South Shetland Islands. *Fish. Sci.* 60, 123–124.

- Kimura, N., Nishimura, A., Tanaka, Y., Yamaguchi, H., 2013. Influence of winter sea-ice motion on summer ice cover in the Arctic. *Polar Res.* 32, 20193.
- Kimura, N., Wakatsuchi, M., 2011. Large-scale processes governing the seasonal variability of the Antarctic sea ice. *Tellus A: Dynamic Meteorology and Oceanography* 63, 828–840.
- Kohlbach, D., Lange, B.A., Schaafsma, F.L., David, C., Vortkamp, M., Graeve, M., van Franeker, J.A., Krumpen, T., Flores, H., 2017. Ice Algae-Produced Carbon Is Critical for Overwintering of Antarctic Krill *Euphausia superba*. *Frontiers in Marine Science* 4.
- Kusahara, K., Hasumi, H., 2013. Modeling Antarctic ice shelf responses to future climate changes and impacts on the ocean. *J. Geophys. Res. Oceans* 118, 2454–2475.
- Kusahara, K., Reid, P., Williams, G.D., Massom, R., Hasumi, H., 2018. An ocean-sea ice model study of the unprecedented Antarctic sea ice minimum in 2016. *Environ. Res. Lett.* 13, 084020.
- Kusahara, K., Williams, G.D., Massom, R., Reid, P., Hasumi, H., 2017. Roles of wind stress and thermodynamic forcing in recent trends in Antarctic sea ice and Southern Ocean SST: An ocean-sea ice model study. *Global Planet. Change* 158, 103–118.
- Kusahara, K., Williams, G.D., Massom, R., Reid, P., Hasumi, H., 2019. Spatiotemporal dependence of Antarctic sea ice variability to dynamic and thermodynamic forcing: A coupled ocean-sea ice model study. *Clim. Dyn.* 52, 3791–3807.
- Loeb, V.J., Santora, J.A., 2015. Climate variability and spatiotemporal dynamics of five Southern Ocean krill species. *Prog. Oceanogr.* 134, 93–122.
- Macdonald, P., Pitcher, T., 1979. Age-groups from size-frequency data: a versatile and efficient method of analyzing distribution mixtures. *Can. J. Fish. Aquat. Sci.* 36, 987–1001.
- Mackintosh, N.A., 1972. Life cycle of Antarctic krill in relation to ice and water conditions. *Discovery Rep.* 36, 1–94.
- Maksym, T., 2019. Arctic and Antarctic sea ice change: contrasts, commonalities, and causes. *Ann. Rev. Mar. Sci.* 11, 187–213.
- Marr, J.W.S., 1962. The natural history and geography of the Antarctic krill (*Euphausia superba* Dana). *Discovery Rep.* 32, 33–464.
- Massom, R.A., Stammerjohn, S.E., 2010. Antarctic sea ice change and variability—physical and ecological implications. *Polar Sci.* 4, 149–186.
- Massom, R.A., Stammerjohn, S.E., Lefebvre, W., Harangozo, S.A., Adams, N., Scambos, T. A., Pook, M.J., Fowler, C., 2008. West Antarctic Peninsula sea ice in 2005: Extreme ice compaction and ice edge retreat due to strong anomaly with respect to climate. *J. Geophys. Res. Oceans* 113.
- Massom, R.A., Stammerjohn, S.E., Smith, R.C., Pook, M.J., Iannuzzi, R.A., Adams, N., Martinson, D.G., Vernet, M., Fraser, W.R., Quetin, L.B., 2006. Extreme anomalous atmospheric circulation in the West Antarctic Peninsula region in austral spring and summer 2001/02, and its profound impact on sea ice and biota. *J. Clim.* 19, 3544–3571.
- Meiners, K.M., Arndt, S., Bestley, S., Krumpen, T., Ricker, R., Milnes, M., Newbery, K., Freier, U., Jarman, S., King, R., Proud, R., Kawaguchi, S., Meyer, B., 2017. Antarctic pack ice algal distribution: Floe-scale spatial variability and predictability from physical parameters. *Geophys. Res. Lett.* 44, 7382–7390.
- Meiners, K.M., Vancoppenolle, M., Thanassekos, S., Dieckmann, G.S., Thomas, D.N., Tison, J.L., Arrigo, K.R., Garrison, D.L., McMinn, A., Lannuzel, D., van der Merwe, P., Swadling, K.M., Smith, W.O., Melnikov, I., Raymond, B., 2012. Chlorophyll *a* in Antarctic sea ice from historical ice core data. *Geophys. Res. Lett.* 39, n/a-n/a.
- Melbourne-Thomas, J., Corney, S., Trebilco, R., Meiners, K., Stevens, R., Kawaguchi, S., Sumner, M., Constable, A., 2016. Under ice habitats for Antarctic krill larvae: Could less mean more under climate warming? *Geophys. Res. Lett.* 43.
- Meredith, M., Sommerkorn, M., Cassotta, S., Derkens, C., Ekyakin, A., Hollowed, A., Kofinas, G., Mackintosh, A., Melbourne-Thomas, J., Muellert, M.M.C., Ottersen, G., Pritchard, H., Schuur, E.A.G., 2019. Polar Regions. In: IPCC Special Report on the Ocean and Cryosphere in a Changing Climate [H.-O. Pörtner, D.C. Roberts, V. Masson-Delmotte, P. Zhai, M. Tignor, E. Poloczanska, K. Mintenbeck, A. Alegría, M. Nicolai, A. Okem, J. Petzold, B. Rama, N.M. Weyer (eds.)].
- Meyer, B., 2012. The overwintering of Antarctic krill, *Euphausia superba*, from an ecophysiological perspective. *Polar Biol.* 35, 15–37.
- Meyer, B., Atkinson, A., Stöbing, D., Oettl, B., Hagen, W., Bathmann, U., 2002. Feeding and energy budgets of Antarctic krill *Euphausia superba* at the onset of winter—I. *Furcilia III* larvae. *Limnol. Oceanogr.* 47, 943–952.
- Meyer, B., Freier, U., Grimm, V., Groeneveld, J., Hunt, B.P., Kerwath, S., King, R., Klaas, C., Pakhomov, E., Meiners, K.M., 2017. The winter pack-ice zone provides a sheltered but food-poor habitat for larval Antarctic krill. *Nat. Ecol. Evol.* 1, 1853–1861.
- Meyer, B., Fuentes, V., Guerra, C., Schmidt, K., Atkinson, A., Spahic, S., Cisewski, B., Freier, U., Olariaga, A., Bathmann, U., 2009. Physiology, growth, and development of larval krill *Euphausia superba* in autumn and winter in the Lazarev Sea, Antarctica. *Limnol. Oceanogr.* 54, 1595–1614.
- Mo, K.C., Higgins, R.W., 1998. The Pacific-South American modes and tropical convection during the Southern Hemisphere winter. *Mon. Weather Rev.* 126, 1581–1596.
- Murphy, E., Johnston, N., Corney, S., Reid, K., 2018. Integrating Climate and Ecosystem Dynamics in the Southern Ocean (ICED) programme: Report of the ICED-CCAMLR Projections Workshop, 5–7 Apr 2018. SC-CAMLR-XXXVII, Hobart, Aus.
- Murphy, E., Thorpe, S., Watkins, J., Hewitt, R., 2004. Modeling the krill transport pathways in the Scotia Sea: spatial and environmental connections generating the seasonal distribution of krill. *Deep Sea Res. Part II* 51, 1435–1456.
- Murphy, E., Watkins, J., Trathan, P., Reid, K., Meredith, M., Thorpe, S., Johnston, N., Clarke, A., Tarling, G., Collins, M., 2007a. Spatial and temporal operation of the Scotia Sea ecosystem: a review of large-scale links in a krill centred food web. *Philos. Trans. R. Soc. Lond. B Biol. Sci.* 362, 113–148.
- Murphy, E.J., Cavanagh, R.D., Drinkwater, K.F., Grant, S.M., Heymans, J., Hofmann, E., Hunt, G.L., Johnston, N.M., 2016. Understanding the structure and functioning of polar pelagic ecosystems to predict the impacts of change. *Proc. R. Soc. B* 283, 20161646.
- Murphy, E.J., Clarke, A., Abram, N.J., Turner, J., 2014. Variability of sea-ice in the northern Weddell Sea during the 20th century. *J. Geophys. Res. Oceans* 119, 4549–4572.
- Murphy, E.J., Trathan, P.N., Watkins, J.L., Reid, K., Meredith, M.P., Forcada, J., Thorpe, S.E., Johnston, N.M., Rothery, P., 2007b. Climatically driven fluctuations in Southern Ocean ecosystems. *Proceedings of the Royal Soc. B: Biol. Sci.* 274, 3057–3067.
- Murphy, E.J., Watkins, J., Reid, K., Trathan, P., Everson, I., Croxall, J., Priddle, J., Brandon, M., Brierley, A., Hofmann, E., 1998. Interannual variability of the South Georgia marine ecosystem: biological and physical sources of variation in the abundance of krill. *Fish. Oceanogr.* 7, 381–390.
- Nicol, S., 2006. Krill, currents, and sea ice: *Euphausia superba* and its changing environment. *AIBS Bulletin* 56, 111–120.
- Nicol, S., Foster, J., 2016. The fishery for Antarctic krill: Its current status and management regime. *Biology and Ecology of Antarctic krill*. Springer 387–421.
- Nicol, S., Pauly, T., Bindoff, N.L., Wright, S., Thiele, D., Hosie, G.W., Strutton, P.G., Woehler, E., 2000. Ocean circulation off east Antarctica affects ecosystem structure and sea-ice extent. *Nature* 406, 504–507.
- Palmer Station Antarctica LTER, Steinberg, D., 2020. Standard body length of *Euphausia superba* collected with a 2-m, 700-um net towed from surface to 120 m, collected aboard Palmer LTER annual cruises off the coast of the Western Antarctic Peninsula, 2009 - 2019, in: Initiative, E.D. (Ed.), 5 ed. Environmental Data Initiative.
- Perry, F.A., Atkinson, A., Sailley, S.F., Tarling, G.A., Hill, S.L., Lucas, C.H., Mayor, D.J., 2019. Habitat partitioning in Antarctic krill: Spawning hotspots and nursery areas. *PLoS ONE* 14, e0219325.
- Piñones, A., Fedorov, A.V., 2016. Projected changes of Antarctic krill habitat by the end of the 21st century. *Geophys. Res. Lett.* 43, 8580–8589.
- Piñones, A., Hofmann, E.E., Daly, K.L., Dinniman, M.S., Klinck, J.M., 2013. Modeling the remote and local connectivity of Antarctic krill populations along the western Antarctic Peninsula. *Mar. Ecol. Prog. Ser.* 481, 69–92.
- Quetin, L.B., Ross, R.M., 2003. Episodic recruitment in Antarctic krill *Euphausia superba* in the Palmer LTER study region. *Mar. Ecol. Prog. Ser.* 259, 185–200.
- Quetin, L.B., Ross, R.M., Fritsen, C.H., Vernet, M., 2007. Ecological responses of Antarctic krill to environmental variability: can we predict the future? *Antarct. Sci.* 19, 253–266.
- R Core Team, 2018. R: A language and environment for statistical computing. R Foundation for Statistical computing, Vienna, Austria.
- Raphael, M.N., 2007. The influence of atmospheric zonal wave three on Antarctic sea ice variability. *Journal of Geophysical Research: Atmospheres* 112.
- Raphael, M.N., Marshall, G., Turner, J., Fogt, R., Schneider, D., Dixon, D., Hosking, J., Jones, J., Hobbs, W.R., 2016. The Amundsen Sea low: Variability, change, and impact on Antarctic climate. *Bull. Am. Meteorol. Soc.* 97, 111–121.
- Saba, G.K., Fraser, W.R., Saba, V.S., Iannuzzi, R.A., Coleman, K.E., Doney, S.C., Ducklow, H.W., Martinson, D.G., Miles, T.N., Patterson-Fraser, D.L., 2014. Winter and spring controls on the summer food web of the coastal West Antarctic Peninsula. *Nat. Commun.* 5, 4318.
- Schaafsma, F., David, C., Pakhomov, E., Hunt, B.P., Lange, B., Flores, H., van Franeker, J. A., 2016. Size and stage composition of age class 0 Antarctic krill (*Euphausia superba*) in the ice-water interface layer during winter/early spring. *Polar Biol.* 39, 1515–1526.
- Schmidt, K., Atkinson, A., Pond, D.W., Ireland, L.C., 2014. Feeding and overwintering of Antarctic krill across its major habitats: The role of sea ice cover, water depth, and phytoplankton abundance. *Limnol. Oceanogr.* 59, 17–36.
- Schmidt, K., Atkinson, A., Steigenberger, S., Fielding, S., Lindsay, M.C., Pond, D.W., Tarling, G.A., Klevjer, T.A., Allen, C.S., Nicol, S., 2011. Seabed foraging by Antarctic krill: Implications for stock assessment, benthopelagic coupling, and the vertical transfer of iron. *Limnol. Oceanogr.* 56, 1411–1428.
- Siegel, V., 2000. Krill (*Euphausiacea*) life history and aspects of population dynamics. *Can. J. Fish. Aquat. Sci.* 57, 130–150.
- Siegel, V., Loeb, V., 1995. Recruitment of Antarctic krill *Euphausia superba* and possible causes for its variability. *Mar. Ecol. Prog. Ser.* 123, 45–56.
- Siegel, V., Watkins, J.L., 2016. Distribution, Biomass and Demography of Antarctic Krill, *Euphausia superba*. In: Siegel, V. (Ed.), *Biology and Ecology of Antarctic Krill*. Springer International Publishing, Cham, pp. 21–100.
- Stammerjohn, S., Martinson, D., Smith, R., Yuan, X., Rind, D., 2008. Trends in Antarctic annual sea ice retreat and advance and their relation to El Niño–Southern Oscillation and Southern Annular Mode variability. *J. Geophys. Res. Oceans* 113.
- Sumata, H., Lavergne, T., Girard-Ardhuin, F., Kimura, N., Tschudi, M.A., Kauker, F., Karcher, M., Gerdes, R., 2014. An intercomparison of Arctic ice drift products to deduce uncertainty estimates. *J. Geophys. Res. Oceans* 119, 4887–4921.
- Szanyi, S., Lukovich, J.V., Barber, D., Haller, G., 2016. Persistent artifacts in the NSIDC ice motion data set and their implications for analysis. *Geophys. Res. Lett.* 43, 10,800–810,807.
- Tamura, T., Ohshima, K.I., Lieser, J.L., Toyota, T., Tateyama, K., Nomura, D., Nakata, K., Fraser, A.D., Jansen, P.W., Newberry, K.B., 2015. Helicopter-borne observations with portable microwave radiometer in the Southern Ocean and the Sea of Okhotsk. *Ann. Glaciol.* 56, 436–444.
- Thorpe, S., Murphy, E., Watkins, J., 2007. Circumpolar connections between Antarctic krill (*Euphausia superba* Dana) populations: investigating the roles of ocean and sea ice transport. *Deep Sea Res. Part I* 54, 792–810.

- Thorpe, S.E., Heywood, K.J., Stevens, D.P., Brandon, M.A., 2004. Tracking passive drifters in a high resolution ocean model: implications for interannual variability of larval krill transport to South Georgia. *Deep Sea Res. Part I* 51, 909–920.
- Thorpe, S.E., Tarling, G.A., Murphy, E.J., 2019. Circumpolar patterns in Antarctic krill larval recruitment: an environmentally driven model. *Mar. Ecol. Prog. Ser.* 613, 77–96.
- Tison, J.-L., Maksym, T., Fraser, A.D., Corkill, M., Kimura, N., Nosaka, Y., Nomura, D., Vancoppenolle, M., Ackley, S., Stammerjohn, S., 2020. Physical and biological properties of early winter Antarctic sea ice in the Ross Sea. *Ann. Glaciol.* 1–19.
- Toyota, T., Ono, S., Cho, K., Ohshima, K.I., 2011. Retrieval of sea-ice thickness distribution in the Sea of Okhotsk from ALOS/PALSAR backscatter data. *Ann. Glaciol.* 52, 177–184.
- Trathan, P.N., Hill, S.L., 2016. The importance of krill predation in the Southern Ocean, *Biology and ecology of Antarctic krill*. Springer 321–350.
- Tschudi, M., Meier, W.N., Stewart, J.S., Fowler, C., Maslanik, J., 2019. Polar Pathfinder Weekly 25 km EASE-Grid Sea Ice Motion Vectors, Version 4, in: Center, N.N.S.a.I.D. C.D.A.A. (Ed.). NASA National Snow and Ice Data Center Distributed Active Archive Center, Boulder, Colorado, USA.
- Turner, J., 2004. The el nino-southern oscillation and antarctica. *Int. J. Climatol.: A J. Royal Meteorol. Soc.* 24, 1–31.
- Veytia, D., Corney, S., Meiners, K.M., Kawaguchi, S., Murphy, E.J., Bestley, S., 2020. Circumpolar projections of Antarctic krill growth potential. *Nat. Clim. Change* 10, 568–575.
- Walsh, J., Reiss, C.S., Watters, G.M., 2020. Flexibility in Antarctic krill *Euphausia superba* decouples diet and recruitment from overwinter sea-ice conditions in the northern Antarctic Peninsula. *Mar. Ecol. Prog. Ser.* 642, 1–19.
- Wiedenmann, J., Cresswell, K.A., Mangel, M., 2009. Connecting recruitment of Antarctic krill and sea ice. *Limnol. Oceanogr.* 54, 799–811.
- Wongpan, P., Meiners, K.M., Langhorne, P.J., Heil, P., Smith, I.J., Leonard, G.H., Massom, R.A., Clementson, L.A., Haskell, T.G., 2018. Estimation of Antarctic Land-Fast Sea Ice Algal Biomass and Snow Thickness From Under-Ice Radiance Spectra in Two Contrasting Areas. *J. Geophys. Res. Oceans* 123, 1907–1923.
- Worby, A.P., Geiger, C.A., Paget, M.J., Van Woert, M.L., Ackley, S.F., DeLiberty, T.L., 2008. Thickness distribution of Antarctic sea ice. *J. Geophys. Res. Oceans* 113.
- Yoshida, T., Kawaguchi, S., Meyer, B., Virtue, P., Penschow, J., Nash, G., 2009. Structural changes in the digestive glands of larval Antarctic krill (*Euphausia superba*) during starvation. *Polar Biol.* 32, 503–507.
- Yuan, X., Li, C., 2008. Climate modes in southern high latitudes and their impacts on Antarctic sea ice. *J. Geophys. Res. Oceans* 113.